Proc. Natl. Acad. Sci. USA
Vol. 91, pp. 8214–8218, August 1994
Cell Biology

Feedback regulation of cell-substratum adhesion by integrin-mediated intracellular Ca^{2+} signaling

(epithelial cells/signal transduction/substrate adhesion)

MICHAEL D. SJAASTAD, BRIGITTE ANGRES, RICHARD S. LEWIS, AND W. JAMES NELSON*

Department of Molecular and Cellular Physiology, Stanford University School of Medicine, Stanford, CA 94305-5426

Communicated by Stanley Falkow, May 2, 1994

ABSTRACT **Integrin binding to extracellular matrix (ECM) regulates cell migration and gene expression in embryogenesis, metastasis, wound healing, and the inflammatory response. In many cases, binding of integrins to ECM triggers intracellular signaling pathways. The regulatory roles of intracellular signaling mechanisms in these events are poorly understood. Using single-cell analysis, we demonstrate that beads coated with peptide containing Arg-Gly-Asp (RGD), an integrin recognition motif found in many ECM proteins, elicit a rapid transient increase in intracellular calcium in Madin–Darby canine kidney (MDCK) epithelial cells. Also, significantly more beads bind to responding cells than to nonresponders. Several independent methods that inhibit RGD-induced Ca^{2+} signaling decrease both the number of beads bound and the strength of adhesion to an RGD-coated substratum. These results indicate that intracellular Ca^{2+} signaling participates in a positive feedback loop that enhances integrin-mediated cell adhesion.**

Interaction of adherent cells with the substratum is mediated by integrin receptors, a family of transmembrane heterodimers that link the cytoskeleton and the cell interior to the extracellular matrix (ECM) (1). The specificity of integrin interaction with various ECM components is conferred by the particular combination of α and β subunits (1, 2). Integrin binding to ECM regulates diverse cellular behaviors, including platelet activation (3, 4), lymphocyte adhesion (5), neutrophil migration (6, 7), endothelial cell spreading and migration (8, 9), and differentiation-specific gene expression (10, 11). It is thought that integrins transduce information from the ECM by triggering intracellular signaling pathways. The pathways may involve mechanical linkages between the ECM and the cytoskeleton (12, 13) and the production of second messengers (8, 9, 14). For example, endothelial cell attachment and spreading on fibronectin or vitronectin triggers independent pathways, resulting in changes in both intracellular free Ca^{2+} concentration ($[Ca^{2+}]_i$) and pH (8, 9). However, there is currently little evidence directly correlating integrin-mediated signal transduction events to specific cellular functions. To address this problem, we have investigated the feedback role of integrin-mediated Ca^{2+} signaling during the initial formation of adhesive cell–substrate contacts by epithelial cells. We used beads coated with a peptide containing the motif Arg-Gly-Asp (RGD), which is recognized by several integrins (1, 2), to examine the induction of Ca^{2+} signaling in single cells and to investigate a role for Ca^{2+} signaling in rapid regulation of integrin-mediated cell adhesion. Our results demonstrate a direct, rapid feedback role for integrin-mediated Ca^{2+} signaling in the strengthening of adhesion of renal epithelial cells to the extracellular matrix.

The publication costs of this article were defrayed in part by page charge payment. This article must therefore be hereby marked "*advertisement*" in accordance with 18 U.S.C. §1734 solely to indicate this fact.

MATERIALS AND METHODS

Cell Culture. Madin–Darby canine kidney (MDCK) epithelial cells were cultured in Dulbecco's modified Eagle's medium (DMEM) with 10% (vol/vol) fetal bovine serum and antibiotics as described (15, 16).

$[Ca^{2+}]_i$ Measurements. Prior to an experiment, a low-density population of single cells was briefly trypsinized and replated on collagen-coated coverslips mounted in viewing chambers for 2–3 hr. Cells were loaded with 2 μM fura-2, acetoxymethyl (AM) ester (Molecular Probes) for 1 hr at 20°C in DMEM lacking phenol red and $NaHCO_3$ and supplemented with 10% fetal bovine serum ($NaHCO_3$ was replaced by 10 mM Hepes and equivalent total osmolarity of the buffer was maintained by adding NaCl); 250 μM sulfinpyrazone was added to all solutions to inhibit dye extrusion (17). Ratio imaging was conducted at 37°C by using a Videoprobe image processor (ETM Systems, Irvine, CA) and an Intensified-charge-coupled device camera (Hamamatsu Photonics, Bridgewater, NJ) coupled to a Zeiss Axiovert 35 microscope with a ×40 objective (Achrostigmat, NA 1.30 oil) as described (18). The RGD-containing peptide, PepTite 2000 (Telios Pharmaceuticals, San Diego), was linked to 2.8-μm tosyl-activated polystyrene magnetic beads (Dynal, Lake Success, NY) as described (19); we call these "RGD-beads." To quantify adhesion, 50 μl of a high-density bead suspension ($\approx 6.5 \times 10^7$ per ml; as seen in *a* of Fig. 1*A*) was added to ensure that all of the cells interacted with at least three beads during the imaging period. Subsequently, cells were photographed before and after a single wash with a stream of buffer ($\approx$0.75 ml at $\approx$0.50 ml/sec) from a pipette (Samco no. 232, San Fernando, CA).

In Ca^{2+} inhibition experiments, cells were simultaneously loaded with 10 μM bis(2-aminophenoxy)ethane-*N*,*N*,*N*′,*N*′-tetraacetate, acetoxymethyl ester (BAPTA, AM) (Molecular Probes) and fura-2 for 1 hr at 20°C. Ni^{2+} was used at 5 mM from a 1 M stock of $NiCl_2$. Low Ca^{2+} medium (LCM) was prepared with dialyzed FBS, resulting in a final concentration of 5 μM Ca^{2+} (16). In both cases, Ni^{2+} and LCM were added 1–2 min prior to the addition of RGD-beads. Thapsigargin (LC Laboratories, Woburn, MA) was prepared as a 1 mM stock solution in dimethyl sulfoxide and was diluted to 1 μM prior to addition to cells. The soluble RGD peptide (H-Gly-Arg-Gly-Asp-Thr-Pro-OH) was purchased from Calbiochem–Novabiochem. The anti-integrin antibodies, LM609 (anti-$\alpha v\beta 3$) and P3G2 (anti-$\alpha v\beta 5$), were provided by David Cheresh (Research Institute of Scripps Clinic, La Jolla, CA). The polyclonal antibody against $\alpha 5\beta 1$ was purchased from

Abbreviations: ECM, extracellular matrix; RGD, Arg-Gly-Asp; MDCK cells, Madin–Darby canine kidney cells; $[Ca^{2+}]_i$, intracellular free calcium concentration; HCM, normal calcium-containing medium (1.8 mM); LCM, low calcium-containing medium (5 μM); BAPTA AM, bis(2-aminophenoxy)ethane-*N*,*N*,*N*′,*N*′-tetraacetate, acetoxymethyl ester; BSA, bovine serum albumin.

*To whom reprint requests should be addressed.

Telios Pharmaceuticals (San Diego). The 3G8 antibody was provided by Warren Gallin (University of Alberta, Canada).

Centrifugal Force-Based Adhesion Assay. The centrifugal force-based adhesion assay was conducted as described (20). Briefly, the wells of 96-well plates were coated with PepTite 2000 (5 μg/ml) at 4°C overnight and blocked with 5% heat-inactivated bovine serum albumin (BSA) for 2 hr at 20°C. MDCK cells were labeled with [^{35}S]methionine (12.5 μCi/ml; 1 μCi = 37 kBq) for 1 hr and incubated in buffer containing 10 mM EDTA for 45 min at 37°C to obtain a single-cell suspension. Cells (2.5×10^4) were added to each well and were centrifuged onto the substratum at $17 \times g$ for 8 min at 20°C. LCM, 5 mM Ni^{2+}, or the monoclonal antibodies (at 1:50 dilution of ascites) were added 1–2 min prior to centrifugation. The plates were inverted and recentrifuged for 8 min at $300 \times g$ to remove nonadherent cells from the substratum. The percentage of adherent cells was calculated by measuring the amount of radioactivity bound to the substratum. In separate experiments, cell contact with RGD-coated coverslips elicited Ca^{2+} transients similar to those of cells in the bead assay, and these transients were inhibited by BAPTA, 5 mM Ni^{2+}, and LCM (data not shown). To achieve a similar inhibition of the $[Ca^{2+}]_i$ increase (as seen in Fig. 2*A*), cells in this assay were preincubated with 15 μM BAPTA, AM for 45 min during the EDTA treatment. Since Ni^{2+} increased background binding of cells to BSA, wells were coated with PepTite 2000 at 8 μg/ml to increase the specific adhesion to RGD. Error bars represent standard deviation of at least four wells. Each experiment was performed two to four times.

RESULTS AND DISCUSSION

Addition of RGD-beads to MDCK epithelial cells preloaded with the Ca^{2+} indicator fura-2 resulted in robust (1000–3000 nM) transient increases in $[Ca^{2+}]_i$ (Fig. 1*A*). The $[Ca^{2+}]_i$ increase occurred ≈20–30 sec after addition of beads. Response latencies overlapped with the time course of bead settling, suggesting that the true response latency following bead–cell contact is <20 sec. After 7–9 min, cells were washed with a stream of buffer to remove nonadherent beads and to show the degree of stable bead–cell binding (*a* and *b* in Fig. 1*A*). Two characteristic responses to RGD-beads were

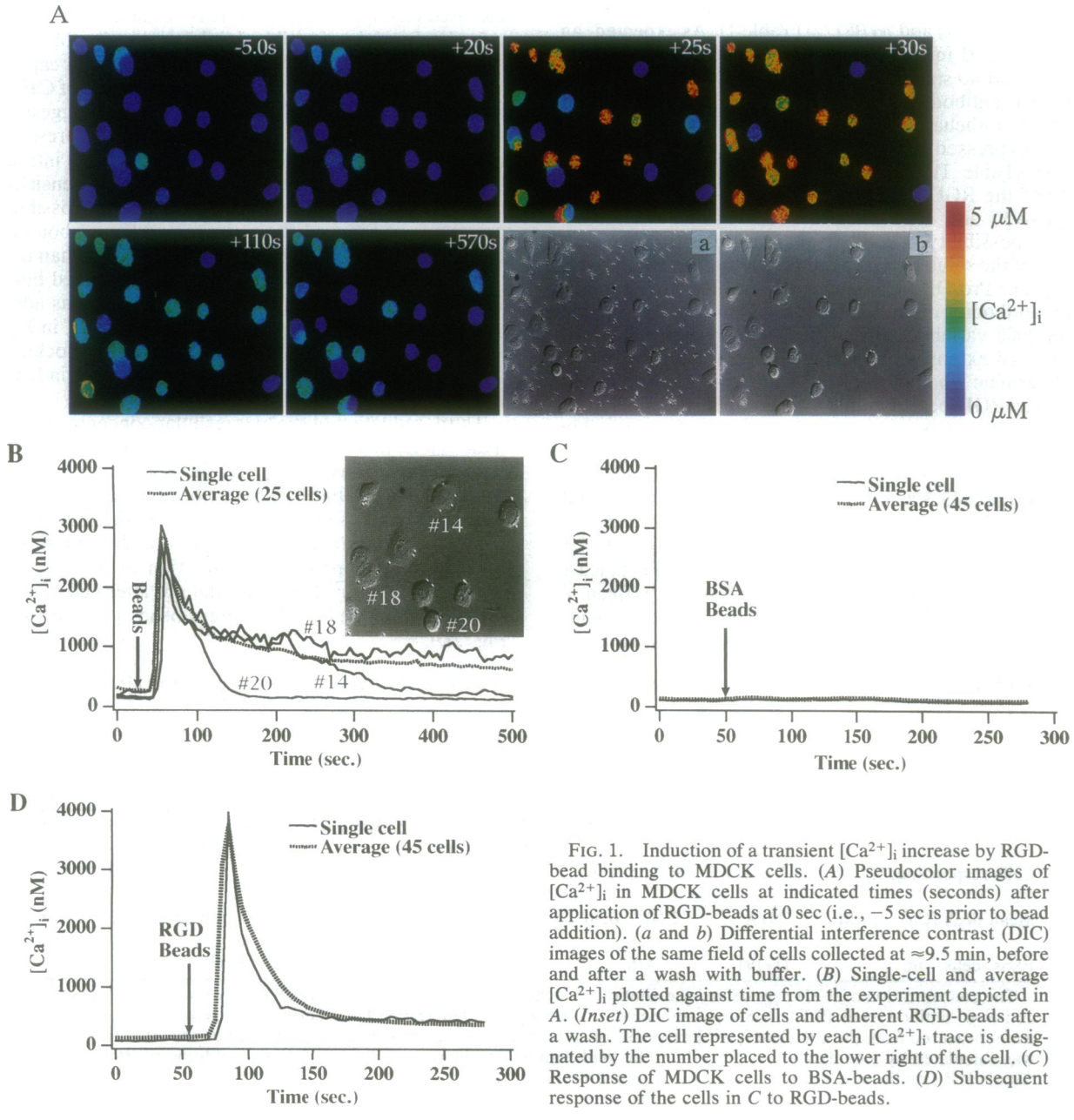

FIG. 1. Induction of a transient $[Ca^{2+}]_i$ increase by RGD-bead binding to MDCK cells. (*A*) Pseudocolor images of $[Ca^{2+}]_i$ in MDCK cells at indicated times (seconds) after application of RGD-beads at 0 sec (i.e., −5 sec is prior to bead addition). (*a* and *b*) Differential interference contrast (DIC) images of the same field of cells collected at ≈9.5 min, before and after a wash with buffer. (*B*) Single-cell and average $[Ca^{2+}]_i$ plotted against time from the experiment depicted in *A*. (*Inset*) DIC image of cells and adherent RGD-beads after a wash. The cell represented by each $[Ca^{2+}]_i$ trace is designated by the number placed to the lower right of the cell. (*C*) Response of MDCK cells to BSA-beads. (*D*) Subsequent response of the cells in *C* to RGD-beads.

observed. In all responding cells, $[Ca^{2+}]_i$ initially increased abruptly from resting levels to 1000–3000 nM (Fig. 1*B*). In approximately half of these cells, the transient was followed by a return to baseline levels (e.g., cells no. 20 and 14). In the remainder of the responders, $[Ca^{2+}]_i$ decreased to a plateau level that was slightly elevated above resting $[Ca^{2+}]_i$ and was sustained for up to 30 min (e.g., cell no. 18). The two response types were not correlated with either cell shape or the number of beads bound.

The transient increase in $[Ca^{2+}]_i$ induced by contact with RGD-beads did not result from mechanical stimulation or nonspecific interaction with protein on the beads. Beads coated with heat-inactivated bovine serum albumin (BSA) did not elicit $[Ca^{2+}]_i$ increases (Fig. 1*C*), nor did they remain bound after a wash with buffer (M.D.S., unpublished observations). However, subsequent addition of RGD-beads evoked robust transient $[Ca^{2+}]_i$ increases in >90% of these cells (Fig. 1*D*), and stable RGD-bead binding was observed (data not shown but similar to *b* of Fig. 1*A*).

The specificity of RGD peptide binding to MDCK cells was further demonstrated by the inhibition of adhesion in cells pretreated with a soluble RGD-containing peptide and monoclonal antibodies that functionally inhibit the RGD-binding integrins, $\alpha v\beta 3$ (21) and $\alpha v\beta 5$ (22) (Table 1). As expected, an antibody to $\alpha 5\beta 1$ integrin, which is not expressed in MDCK cells (27), had no significant effect on RGD-bead binding. A monoclonal antibody directed against the extracellular domain of the epithelial cell–cell adhesion molecule E-cadherin, which is expressed in MDCK cells, failed to inhibit RGD adhesion (Table 1). From these data, we conclude that binding of the RGD-beads is specific and occurs primarily through $\alpha v\beta 3$ and $\alpha v\beta 5$ integrins, although we cannot exclude the possibility that other integrins are also involved. Addition of the soluble RGD peptide (200 μg/ml; H-Gly-Arg-Gly-Asp-Thr-Pro-OH, Calbiochem–Novabiochem) or anti-integrin antibodies did not induce $[Ca^{2+}]_i$ increases. Soluble PepTite 2000 variably induced $[Ca^{2+}]_i$ increases and, thus, was not used extensively for competition studies.

To determine whether the $[Ca^{2+}]_i$ increase was correlated with stable RGD-bead binding, we grouped the single-cell analysis of 10 independent experiments into four possible bead–response combinations: cells that bound beads and had a $[Ca^{2+}]_i$ increase (57.7 ± 6.8%; $Bead^+/Ca^{hi}$) or lacked a $[Ca^{2+}]_i$ increase (13.3 ± 5.0%; $Bead^+/Ca^{lo}$) and cells that did not bind beads and had a $[Ca^{2+}]_i$ increase (15.2 ± 5.4%; $Bead^-/Ca^{hi}$) or lacked a $[Ca^{2+}]_i$ increase (13.8 ± 3.3%; $Bead^-/Ca^{lo}$). The results of this analysis show that in at least some cells, a $[Ca^{2+}]_i$ increase was neither necessary ($Bead^+/Ca^{lo}$) nor sufficient ($Bead^-/Ca^{hi}$) to induce stable bead binding. However, >80% of all $Bead^+$ cells were also Ca^{hi}, demonstrating that the $[Ca^{2+}]_i$ increase is strongly correlated with bead binding. In addition, significantly more beads bound to the cells that had a $[Ca^{2+}]_i$ increase (3.02 ± 0.44 beads per cell) than bound to nonresponding cells (1.36 ± 0.5; $P < 0.023$, unpaired *t* test). If one assumes that every cell interacts with at least three beads (Fig. 1*A*), this finding strongly suggests that the increase in $[Ca^{2+}]_i$ enhances the probability of stable bead binding.

We tested whether the Ca^{2+} transient was causal in the enhancement of bead binding. First, cells were preloaded with the cell-permeant calcium chelator BAPTA, AM, which slowed the time course and reduced the magnitude of the $[Ca^{2+}]_i$ increase elicited by RGD-beads (Fig. 2*A*; compare with Fig. 1*B*). BAPTA also significantly inhibited the binding of RGD-beads (Fig. 2*D*).

Second, pretreatment of cells with 5 mM Ni^{2+} for 1–2 min almost completely abolished the $[Ca^{2+}]_i$ increase induced by RGD-beads (Fig. 2*B*); 5 mM Ni^{2+} blocks many types of Ca^{2+} channels, including depletion-activated Ca^{2+} channels (23–25). One micromolar thapsigargin (a microsomal Ca^{2+}-ATPase inhibitor that depletes intracellular Ca^{2+} stores) stimulated a transient increase in $[Ca^{2+}]_i$ followed by an elevated plateau (≈1000 nM). This sustained component was completely and reversibly inhibited by 5 mM Ni^{2+} (not shown), suggesting that MDCK cells possess a capacitative Ca^{2+} entry pathway activated by the depletion of Ca^{2+} stores as described in other cells (23–25). Thus, we suggest that the small $[Ca^{2+}]_i$ transients that remained in the presence of 5 mM Ni^{2+} likely represent Ca^{2+} release from intracellular stores. However, the operation of other Ni^{2+}-sensitive Ca^{2+} channels in the RGD-bead response is also possible. Ni^{2+} pretreatment reduced the average number of bound RGD-beads to the level of nonresponding cells (less than one bead per cell; see Fig. 2 *B Inset* and *D*). The reduced binding of RGD-beads did not occur when 5 mM Ni^{2+} was added 7–9 min after the Ca^{2+} transient [see "Ni^{2+} (post)" in Fig. 2*D*), suggesting that Ni^{2+} inhibited adhesion by blocking Ca^{2+} influx and not by functional disruption of integrin binding to RGD.

Third, reduction of the extracellular concentration of Ca^{2+} ($[Ca^{2+}]_o$) from 1.8 mM (HCM) to 5 μM (LCM) significantly reduced both the average size of the $[Ca^{2+}]_i$ increase (Fig. 2*C*) and the average number of bound beads (Fig. 2*D*). Small Ca^{2+} transients were sometimes evident in these experiments, possibly representing Ca^{2+} store release (data not shown). As with the Ni^{2+} experiments, reduction of $[Ca^{2+}]_o$ after the RGD-induced $[Ca^{2+}]_i$ increase did not alter cell morphology or reduce the number of adherent beads ["LCM (post)" in Fig. 2*D*].

Table 1. RGD-bead binding and Ca^{2+} responses in MDCK cells under normal and inhibitor conditions in MDCK cells

	Beads		Pretreatment			
			Soluble RGD	Antibody		
Measurement	BSA	RGD	(200 μg/ml)	3G8 (1:50)	αvβ3 (1:100)	αvβ5 (1:100)
Beads per cell, no.	0.0 ± 0.0	2.70 ± 1.25	0.76 ± 0.37 *(*P* = 0.015)	2.63 ± 1.67	0.60 ± 0.62 *(*P* = 0.06)	0.68 ± 0.58 *(*P* = 0.034)
Cells responding, %	8.3 ± 8.5	96.5 ± 4.0	80.2 ± 9.2 *(*P* = 0.013)	87.7 ± 12.3	88.3 ± 7.7	93.0 ± 4.7
Mean peak $[Ca^{2+}]_i$, μM	N/A	2.00 ± 0.30	2.04 ± 0.74	1.62 ± 0.69	1.44 ± 0.69	1.33 ± 0.46 *(*P* = 0.036)
Exps. cells,† no.	11/191	4/67	5/113	7/74	3/47	4/54

The concentration of RGD peptide and the dilution of ascites are indicated. The anti-αvβ3 antibody was LM609 and the anti-αvβ5 antibody was P3G2. 3G8 was a monoclonal antibody directed against E-cadherin. Average peak $[Ca^{2+}]_i$ values were measured from the averaged $[Ca^{2+}]_i$ response of all cells in each experiment. The percentage of cells that responded was calculated by including all of the cells in the field with $[Ca^{2+}]_i$ increases of >500 nM after addition of RGD beads.
*Statistical significance was tested with the unpaired Student *t* test.
†Ratio of total number of experiments to total number of cells used.

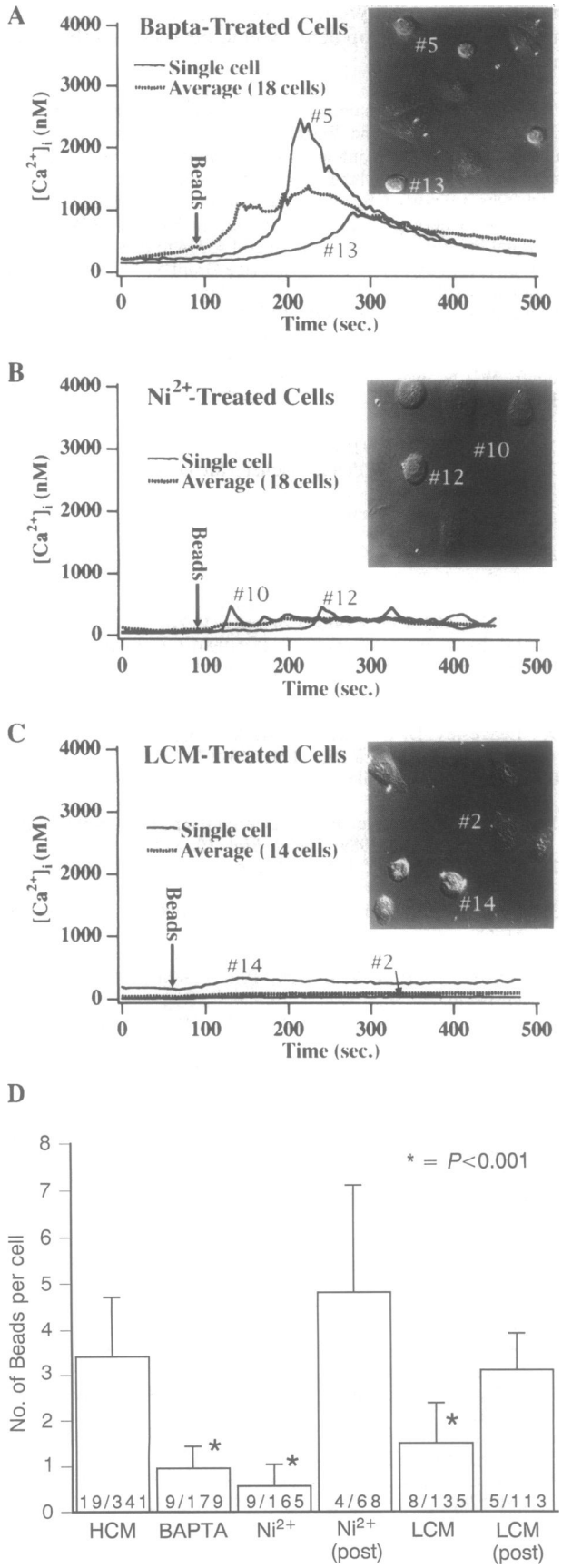

FIG. 2. Inhibition of the RGD-induced $[Ca^{2+}]_i$ increase in MDCK cells reduces the strength of cell adhesion. (*Insets* in *A*, *B*, and *C*) DIC images of RGD-beads bound to cells after washing with buffer 7–9 min after adding beads. The cell represented by each $[Ca^{2+}]_i$ trace is designated by the number placed to the lower right of the cell (except cell no. 2 in *C*, for which the number is to the left of the cell). (*A*) Response of BAPTA, AM-loaded cells. (*B*) Response of cells pretreated 1–2 min with 5 mM Ni^{2+}. (*C*) Response of cells pretreated 1–2 min. with LCM ($\approx$5 μM $[Ca^{2+}]_o$). (*D*) The average number of beads bound per cell under the different experimental conditions used in *A*, *B*, and *C*; fractions within each bar indicate the number of individual experiments and cells analyzed, respectively; statistical significance was tested with the unpaired Student *t* test. Error bars represent SDs.

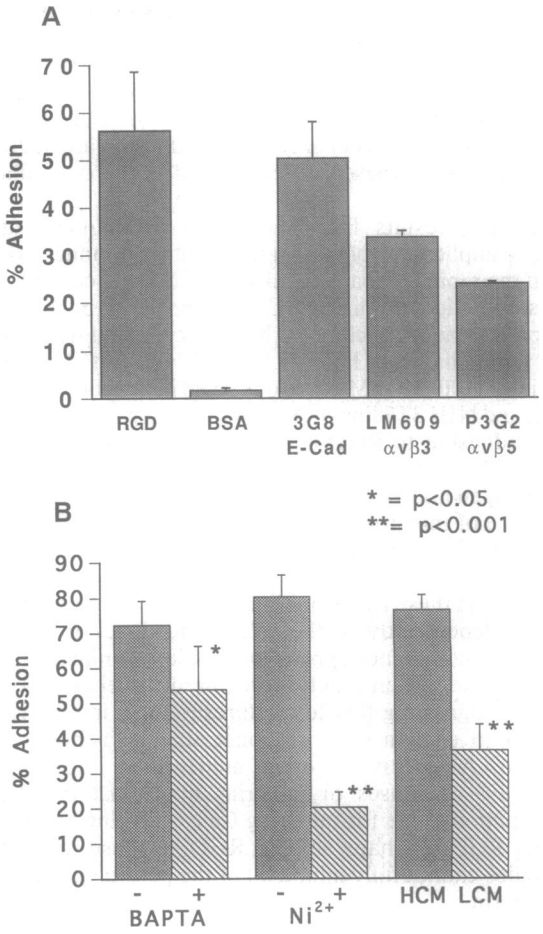

FIG. 3. Cell adhesion to an RGD-coated substratum measured in a centrifugal force-based adhesion assay. (*A*) Adhesion to an RGD- or BSA-coated substratum, or to RGD in the presence of monoclonal antibodies directed against E-cadherin (E-cad), $\alpha v\beta 3$, or $\alpha v\beta 5$ integrins. (*B*) Cell adhesion to an RGD-coated substratum after inhibition of the $[Ca^{2+}]_i$ increase by BAPTA, 5 mM Ni^{2+}, or LCM. Statistical significance was tested with the unpaired Student *t* test. Error bars represent SDs.

In summary, inhibition of the RGD-bead-induced $[Ca^{2+}]_i$ increase by three independent methods resulted in a significant reduction in binding of RGD-beads to cells, suggesting that the rapid stabilization of initial RGD-integrin interactions requires Ca^{2+} influx across the plasma membrane.

To investigate whether a similar Ca^{2+}-dependent feedback mechanism regulates the strength of cell binding to RGD-coated substratum, we used a quantitative adhesion assay in which a defined centrifugal force is applied to attached cells (Fig. 3). In these experiments, we followed a similar time course and applied the same conditions that were used to inhibit $[Ca^{2+}]_i$ increases in the bead-binding assay. Cell adhesion to an RGD-coated substratum was competitively inhibited by monoclonal antibodies against $\alpha v\beta 3$ and $\alpha v\beta 5$ integrins, while antibodies to E-cadherin had no effect (Fig. 3*A*). Soluble RGD also inhibited adhesion in three of five

experiments with this assay (data not shown). As in the bead-binding experiments, BAPTA, 5 mM Ni^{2+}, and LCM reduced adhesion to the RGD-coated substratum (Fig. 3*B*), suggesting a similar role for the $[Ca^{2+}]_i$ increase in regulation of substrate adhesion. However, it is also possible that slightly different aspects of substrate adhesion are addressed by the different types of force applied in the two adhesion assays.

Together, results from these two independent assays strongly implicate a role for an RGD/integrin-induced $[Ca^{2+}]_i$ rise in the rapid feedback regulation of MDCK cell adhesion. The stimulation of similar $[Ca^{2+}]_i$ transients by RGD was observed in another clone of MDCK cells and in two other renal epithelial cell lines, LLCPK1 and IMCD. Smaller transients (100–300 nM) were observed in fibroblasts (L cells, Rat-2, and NIH 3T3 lines). At least two integrins are involved in the adhesion to RGD and the Ca^{2+} response, $\alpha v\beta 3$ and $\alpha v\beta 5$, both of which are expressed in adult murine kidney (P. Piepenhagen and W.J.N., unpublished observations). Steric hindrance of integrin–RGD binding by soluble RGD or pretreatment with anti-integrin antibodies reduced adhesion but did not reduce the $[Ca^{2+}]_i$ increase to the same extent. This suggests that these agents inhibit adhesion at the cell surface, acting independently of the calcium feedback mechanism. However, they do not appear to completely inhibit the level of RGD–integrin interaction required to elicit Ca^{2+} responses, suggesting that lower thresholds of interaction are required to elicit a Ca^{2+} response than to achieve stable adhesion. Alternatively, other unidentified integrins may elicit Ca^{2+} responses or integrins may exist in different conformations, one for initiating Ca^{2+} signaling and one for binding RGD. Perhaps soluble RGD or these monoclonal antibodies cannot fully inhibit all of the possible functions of the integrin.

The design of the single-cell and cell-population analyses enabled us to correlate cellular responses with integrin–RGD binding over a very short time course (<10 min). The important finding of this study is that specific integrin–ECM interactions induce an immediate Ca^{2+} signal that results in the rapid strengthening of adhesion. However, inhibition of the $[Ca^{2+}]_i$ increase did not decrease bead binding when the beads were left on cells for >30 min (M.D.S. and W.J.N., unpublished observations). This long-term, Ca^{2+}-independent response has been reported previously for endothelial cells binding to fibronectin (26). We suggest that integrin/RGD-induced Ca^{2+}-signaling accelerates the kinetics of this long-term response resulting in an immediate strengthening of adhesion. It is possible that additional intracellular signals (kinases, phosphatases) acting in concert with the $[Ca^{2+}]_i$ increase play a role in the regulation of adhesion. The mechanisms involved in stabilization of adhesion may involve conformational changes in the integrin binding site for RGD (4), integrin clustering, or rapid assembly of the cytoskeleton to form a focal adhesion contact (12, 19). In this context, it is noteworthy that bead binding, but not the transient increase in $[Ca^{2+}]_i$, is inhibited by disruption of the actin cytoskeleton by cytochalasin D (M.D.S. and W.J.N., unpublished observations). This indicates that an intact actin cytoskeleton is not required for the immediate Ca^{2+}-signaling response, but it is required for stable adhesion. We suggest that rapid Ca^{2+}-mediated regulation of cell adhesion to the ECM may be physiologically important at times when cells must respond rapidly during, for example, exploratory cell movements in development, wound healing, and the inflammatory response.

The first two authors contributed equally to this study. We thank Drs. David Cheresh and Warren Gallin for supplying monoclonal antibodies specific for integrins and E-cadherin, respectively, and members of the Nelson lab for critically reading the manuscript. This work was supported by National Institutes of Health Grant GM 35527 and American Cancer Society Grant BE-144 to W.J.N. and National Institutes of Health Grant GM 45374 to R.S.L. M.D.S. was also supported by Public Health Service Grant 5T32CA09302-16 and National Institutes of Health Fellowship F32 GM16331, and B. Angres was supported by a fellowship from the North Atlantic Treaty Organization administered through the Deutscher Akademischer Austauschdienst, and a fellowship from the Forschungsgemeinschaft. W.J.N. was an Established Investigator of the American Heart Association.

1. Hynes, R. O. (1992) *Cell* **69**, 11–25.
2. Rouslahti, E. & Pierschbacher, M. D. (1987) *Science* **238**, 491–497.
3. Phillips, D. R., Charo, I. F. & Scarborough, R. M. (1991) *Cell* **65**, 359–362.
4. Du, X., Plow, E. F., Frelinger, A. L., III, O'Toole, T. E., Loftus, J. C. & Ginsburg, M. H. (1991) *Cell* **65**, 409–416.
5. Kooy, Y. V., Weder, K. P., Heije, K., Malefijt, R. & Figdor, C. G. (1993) *Cell Adhes. Commun.* **1**, 21–32.
6. Marks, P. W. & Maxfield, F. R. (1990) *J. Cell Biol.* **110**, 43–52.
7. Hendey, B., Klee, C. B. & Maxfield, F. R. (1992) *Science* **258**, 296–299.
8. Schwartz, M. A. (1993) *J. Cell Biol.* **120**, 1003–1010.
9. Leavesley, D. I., Schwartz, M. A., Rosenfeld, M. & Cheresh, D. A. (1993) *J. Cell Biol.* **121**, 163–170.
10. Streuli, C. H., Bailey, N. & Bissell, M. J. (1991) *J. Cell Biol.* **115**, 1383–1395.
11. Werb, Z., Tremble, P. M., Behrendtsen, O., Crowley, E. & Damsky, C. H. (1989) *J. Cell Biol.* **10**, 877–889.
12. Wang, N., Butler, J. P. & Ingber, D. E. (1993) *Science* **260**, 1124–1127.
13. Bissell, M. J., Hall, H. G. & Parry, G. (1982) *J. Theor. Biol.* **99**, 31–68.
14. Schwartz, M. A. (1992) *Trends Cell Biol.* **2**, 304–308.
15. Nelson, W. J. & Veshnock, P. J. (1986) *J. Cell Biol.* **103**, 1751–1765.
16. Nelson, W. J. & Veshnock, P. W. (1987) *J. Cell Biol.* **104**, 1527–1537.
17. Di Virgilio, F., Steinberg, T. H. & Silverstein, S. C. (1990) *Cell Calcium* **11**, 57–62.
18. Lewis, R. S. & Cahalan, M. D. (1989) *Cell Regul.* **1**, 99–112.
19. Plopper, G. & Ingber, D. E. (1993) *Biochem. Biophys. Res. Commun.* **193**, 571–578.
20. Lotz, M. M., Burdsal, C. A., Erickson, H. P. & McClay, D. R. (1989) *J. Cell Biol.* **109**, 1795–1805.
21. Cheresh, D. A. & Spiro, R. C. (1987) *J. Biol. Chem.* **262**, 17703–17711.
22. Wayner, E. A., Orlando, R. A. & Cheresh, D. A. (1991) *J. Cell Biol.* **113**, 919–929.
23. Zweifach, A. & Lewis, R. S. (1993) *Proc. Natl. Acad. Sci. USA* **90**, 6295–6299.
24. Matthews, G. E., Neher, E. & Penner, R. J. (1989) *J. Physiol. (London)* **418**, 105–130.
25. Hallam, T. J., Jacob, R. & Merrit, J. E. (1988) *Biochem J.* **255**, 179–184.
26. Schwartz, M. A., Brown, E. J. & Fazeli, B. (1993) *J. Biol. Chem.* **268**, 19931–19934.
27. Ojakian, G. K. & Schwimmer, R. (1994) *J. Cell Sci.* **107**, 561–576.